

## Hole Burning Effects in a He-Ne Optical Maser

W. R. BENNETT, JR.

*Bell Telephone Laboratories, Murray Hill, New Jersey*

(Received November 20, 1961)

A study has been made of pulling effects by the amplifying media on the  $TEM_{00}$  modes of a helium-neon maser using a circular plane mirror Fabry-Perot cavity in which the mirror separation was known with precision. Approximate expressions are derived for mode pulling in homogeneously and inhomogeneously broadened optical masers. The experimental results suggest that the losses in the maser are not determined entirely by the mirror reflectance coefficient. A power-dependent splitting of the beat frequencies between simultaneously oscillating modes is explained in terms of a nonlinear frequency-dependent pulling effect arising from inhomogeneous broadening. The case of Lorentzian holes

burned in a Gaussian line is treated specifically. It is suggested that the anomalous variation of beat frequencies with pumping rate results from hole repulsion effects and that the hole widths required arise from the combined effects of small-angle elastic scattering and stimulated emission. It is a consequence of the interpretation that the number of simultaneously oscillating even-symmetric modes in the helium-neon maser may easily be determined from the Fourier spectrum of the beat frequencies. A method is described by which the central cavity resonance may be stabilized near the center of the Doppler line in the case of three oscillating symmetric modes.

### 1. INTRODUCTION

THE narrow linewidths inherent in the helium-neon optical maser<sup>1,2</sup> are suggestive of a number of basic experiments. However, the ultimate usefulness of this narrow source of radiation, both as a research tool and a communications device, is largely limited by the frequency stability that may be obtained. For the latter reason, the present investigation was undertaken. Since the oscillation frequencies are primarily determined by the cavity resonances, and therefore the dimensions of the maser, it was not obvious *a priori* that a long-term frequency stability of much better than half the separation between adjacent cavity resonances (about 80 Mc/sec) could actually be obtained. It became apparent during the course of this research, however, that a method existed by which one could both determine the number of simultaneously oscillating modes and, in the case of three oscillations, set the central mode near the center of the Doppler line. The absolute stability that may be achieved in this way is still unknown and is currently under investigation. It seems clear that the method may at least be used to obtain an extremely high degree of relative stability.

### 2. MASER CONSTRUCTION

For the purpose of making the present study, the He-Ne maser shown in Fig. 1 was constructed. The mechanical design of the interferometer was altered from that of the original He-Ne maser,<sup>1</sup> in order to minimize mechanical fluctuations and permit an accurate determination of the plate separation. Each of the Fabry-Perot plates was fastened by spring clips to internal three-point mountings which, in turn, were securely fastened to the large external flanges shown at either end of the maser. The large flanges were surface-ground and separated by four 1-in. diameter Nilvar rods, cut to

lengths which were identical within 0.0005 in. The bellows incorporated at each end of the discharge tube were sufficiently flexible to permit changing the plate separation by about 4.5% through the insertion of accurately machined spacers at the ends of the 1-in. diameter rods. Of several methods tried for controlling the plate angular alignment, one based on the magnetostrictive effect in the Nilvar supporting rods was found to be the most satisfactory. The magnetostrictive effect was also found to present a convenient method for changing the plate separation; however, with the adjustments used, some coupling between the plate separation and angular alignment controls existed. A more detailed description of the alignment method and interferometer construction will be given elsewhere. The improved mechanical stability obtained with the present maser arises largely by virtue of the fact that the tuning is accomplished through the slight distortion of a highly rigid structure. In other respects, the maser had properties similar to those reported in the first He-Ne maser with the exception that the device oscillated only on the strongest ( $2s_2$  to  $2p_4$  in Paschen notation at 11 522.76 Å)<sup>3</sup> of the five transitions of neon previously observed. The plates used were flat to  $\cong \lambda/100$  over the beam diameter and had a reflectance of 99% at the wavelength used prior to insertion in the maser.<sup>4</sup>

### 3. EXPERIMENTAL RESULTS

The modes of oscillation were studied by observing the difference frequencies produced when light from the maser was focussed on the surface of a 7102 photomultiplier tube. The photosurface acts as a square-law detector and one may observe all possible difference frequencies up to the maximum frequency response characteristic of the tube. This effect was first observed

<sup>1</sup> A. Javan, W. R. Bennett, Jr., D. R. Herriott, Phys. Rev. Letters **6**, 106 (1961).

<sup>2</sup> A. Javan, E. A. Ballik, and W. L. Bond (to be published) have recently remeasured the linewidths in the first maser and have found that they are inherently in the order of 2 cycles/sec or less.

<sup>3</sup> The author is indebted to D. L. Wood for his help in firmly establishing the identity of this line. The small possibility that the strongest maser transition might have been the  $2s_4-2p_7$  line at 11 525.016 Å had not previously been ruled out experimentally.

<sup>4</sup> The author is indebted to D. R. Herriott for making these measurements.

by Forrester, Gudmundsen, and Johnson<sup>5</sup> using incoherent light sources and more recently was used to investigate the linewidths obtained in the first helium-neon maser.<sup>1,2</sup> A previous report on the difference-frequency spectrum obtained in this way from a He-Ne maser has been given by Herriott<sup>6</sup> and, for the sake of clarity, will be summarized here. Since the single-pass gain obtainable from a He-Ne maser is small, one is forced to use a Fabry-Perot cavity with an enormously high  $Q$  in order to exceed the threshold requirement for oscillation. In practice this implies a cavity width which is much narrower than the Doppler width for one transition and that the frequencies of oscillation will be primarily determined by the cavity resonances. The dominant cavity resonance frequencies are determined by requiring that the cavity length  $L$  be a half-integral multiple of the wavelength. These resonant frequencies correspond to the first even-symmetric radial modes calculated by Fox and Li<sup>7</sup> and differ in frequency by  $c/2L \cong 160$  Mc/sec for the present work, where  $c$  is the velocity of light in vacuum. Since these frequency separations are small compared to the Doppler width, the maser may oscillate on several of these frequencies simultaneously. In addition to the even-symmetric modes, Fox and Li have shown that the next longitudinal modes of importance are those possessing odd radial symmetry and that these differ from the former by frequencies of the order of a Mc/sec with the present geometry. Hence, as was reported by Herriott,<sup>6</sup> one obtains a difference frequency spectrum of the type shown in Fig. 2. That is, a peak at zero frequency corresponding to each line beating with itself, followed by a peak  $\cong 1$  Mc/sec away corresponding to all possible differences between the first even- and odd-symmetric radial modes having the same value of  $c/2L$ ; a peak at  $c/2L$  corresponding to the differences between all even-symmetric modes separated by  $c/2L$  and all odd-symmetric modes separated by  $c/2L$ , surrounded by two satellites corresponding to the possible even-odd and odd-even difference frequencies at approximately  $c/2L$ , etc. As indicated by the arrows in Fig. 2, the satellites obtained as a result of the beats between the odd-even

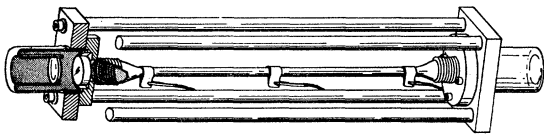


FIG. 1. He-Ne optical maser used. The "cut-away" section at the left shows the location of the exit window and Fabry-Perot plate. The discharge is driven by a 30-Mc/sec (20 to 50 watt) supply through the three external electrodes shown. The plate separation and angular alignment is controlled magneto-strictively by coils (not shown) placed about each of the four Nilvar supporting rods.

<sup>5</sup> A. T. Forrester, R. A. Gudmundsen, and P. O. Johnson, *Phys. Rev.* **99**, 1691 (1955).

<sup>6</sup> D. R. Herriott, in *Advances in Quantum Electronics*, edited by J. R. Singer (Columbia University Press, New York, 1961), p. 49.

<sup>7</sup> A. G. Fox and Tingye Li, *Bell System Tech. J.* **40**, 453 (1961).

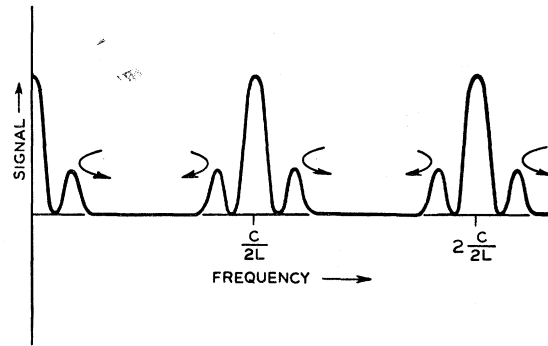


FIG. 2. Fourier spectrum from possible difference frequencies in the maser.

symmetric modes vary strongly with the interferometer plate alignment, reaching a minimum separation from the  $c/2L$  beats at parallel alignment. For the latter reason, they are both easily identifiable, and unsuitable for the present study. The discussion which follows is concerned entirely with the central peaks obtained at multiples of  $c/2L$  corresponding to the differences between the even-symmetric modes. That is, the low power data were taken under conditions where the satellites about the  $c/2L$  and  $2(c/2L)$  were absent.

The light output of the maser was found to have more or less random polarization. The output varied from the extreme case of linear polarization with arbitrary orientation of the electric field vector to nearly perfect circular polarization over time intervals in the order of seconds. This result would be expected from ideal cylindrical geometry and is in contrast with the behavior of the first He-Ne maser.<sup>1,8</sup> In addition, the various modes of oscillation in the present maser were also found to have unrelated polarizations. The latter was established by examining the behavior of the beat frequencies when a linear polaroid was inserted in the beam. Javan and Ballik<sup>9</sup> have observed that the central  $c/2L$  beat may sometimes not be observable without the use of a polaroid. Their observation may be interpreted through the assumption that the two modes producing the beat are polarized linearly at right angles. The phototube, being a reasonably good square-law detector, fails to respond to the beat since the difference frequency is contained in the scalar product of the two electric fields. The insertion of a polaroid at  $45^\circ$  to the field components, however, restores the beat. That is, the polaroid transmits components of the two fields which are parallel. In order to avoid missing any of the beats in the present work, a polaroid was always inserted in the beam and rotated until a location was obtained in which all beats present were observed with comparable

<sup>8</sup> The first He-Ne maser was linearly polarized in a direction closely correlated with a striated pattern in the dielectric coatings. The absence of such striated patterns in the present maser may have resulted from the use of more modest bake-out temperatures.

<sup>9</sup> A. Javan and E. A. Ballik (private communication).

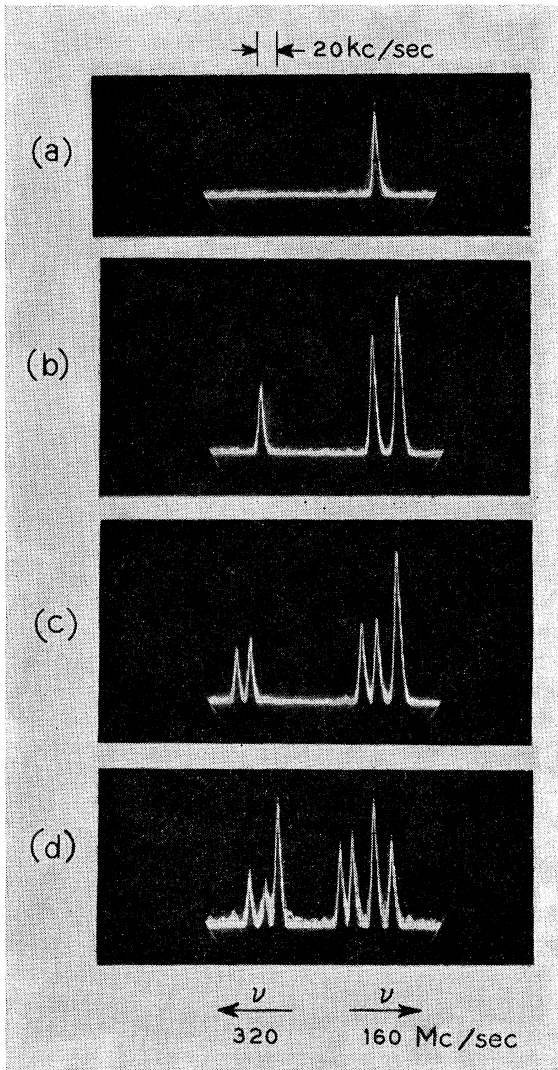


FIG. 3. Splitting of  $c/2L$  and  $2(c/2L)$  beats with power. Power increases from (a) to (d).

amplitude. For this reason, the relative amplitudes (for example of the split components in Fig. 3) are arbitrary.

The first measurements were made on the absolute frequency of the central peak corresponding to a difference frequency of  $c/2L$ . These measurements were made under the conditions of low power in which this beat was not split and the beat at  $2c/2L$  was not observable, i.e., the conditions under which the data in Fig. 3(a) were taken. Measurements were made at three discrete interferometer lengths and these data are shown in Table I. The uncertainty in the absolute frequency measurement ( $\cong 20$  kc/sec) arises primarily from the variation of the beat frequency with power and plate separation as discussed below. As is obvious from Table I, the beat frequency is not equal to  $c/2L$ , but is less than  $c/2L$  by about 1 part in 800. This effect may be readily explained on the basis of mode pulling by the

TABLE I. Comparison of measured beat frequencies with the difference between calculated cavity resonance frequencies for three separate cavity lengths.

$c/2L$ (in Mc/sec)	Measured beat (in Mc/sec)	Fractional difference between $c/2L$ and measured beat
$161.316 \pm 0.022$	$161.107 \pm 0.010$	$-(1.3 \pm 0.2) \times 10^{-3}$
$158.713 \pm 0.020$	$158.531 \pm 0.010$	$-(1.1 \pm 0.2) \times 10^{-3}$
$156.189 \pm 0.018$	$155.982 \pm 0.010$	$-(1.3 \pm 0.2) \times 10^{-3}$

Doppler line and is discussed in Sec. 13. It is a consequence of the analysis in Sec. 5 and the data in Table I that the loss in the interferometer exceeds the known reflectance loss by a factor of about two.

There are two interesting aspects of the data obtained at increasing power levels:

(a) The frequency of the  $c/2L$  beat was found to increase with increasing power. The magnitude of the increase before splitting occurred (see below) was dependent on the setting of the interferometer plates. It varied from nearly zero to a maximum of about 30 kc/sec. As will become evident from the analysis in Sec. 5, such an increase is anomalous. That is, for any singly-peaked line one would expect the pulling towards the line center to increase with the number of excited atoms and that the pulling would be less for a cavity resonance near the line center than for one farther away from it. Hence one would expect the frequency separation between adjacent cavity resonances to decrease with increasing power. The same anomalous behavior was encountered in the split components described below. The anomaly is explained through the hole repulsion effect in Sec. 13.

(b) A power-dependent splitting of the  $c/2L$  and  $2(c/2L)$  beats was encountered. Figs. 3(a) through 3(d) show data taken simultaneously on the central beats at both  $c/2L$  and  $2(c/2L)$  with increasing rf power. The data on the right show the  $c/2L$  beat (160 Mc/sec) and those on the left the  $2(c/2L)$  beat (320 Mc/sec). The frequency scale is the same in each case as indicated by the 20 kc/sec interval shown, with the exception that increasing frequency occurs in opposite directions for the two sets of data. These data were taken by adjusting the maser length so that the  $c/2L$  beat occurred within the first if band of the spectrum analyzer used and by tuning the local oscillator in the analyzer to correspond to the  $2(c/2L)$  beat. The data shown in Figs. 3(a) through 3(d) were taken at increasing power levels, where each figure represents about 10 oscilloscope traces. In Fig. 3(a) the  $c/2L$  beat is present and the  $2(c/2L)$  beat is not. As the power increases [Fig. 3(b)], the  $c/2L$  beat splits by an amount which typically was in the order of 20 kc/sec and the  $2(c/2L)$  beat appears. The separation between the two ( $c/2L$ ) components in Fig. 3(b) was dependent on the interferometer length. By changing the plate separation magnetostrictively, the splitting shown in Fig. 3(b) could be varied from a

maximum of about 30 kc/sec to a minimum of  $\leq 1$  kc/sec (i.e., 1 kc/sec was the minimum if resolution of the apparatus used). With a further increase in power [Fig. 3(c)], the  $c/2L$  beat breaks into three components and the beat at  $2(c/2L)$  splits. Again the frequency of the components was found to increase with power and the splitting was dependent on the interferometer setting. For some interferometer settings, the odd-symmetric modes (as evidenced by the appearance of the satellites in Fig. 2) were also present during conditions typical of Fig. 3(c). Their presence or absence seemed to have relatively little effect on the splitting of the central  $c/2L$  and  $2(c/2L)$  beats. Finally, at the highest power level shown in Fig. 3, the  $c/2L$  beat has broken into four components and the  $2(c/2L)$  beat into three.

The data in Fig. 3 may be interpreted in the following way: Some nonlinear frequency-dependent pulling mechanism exists whereby the differences between adjacent oscillating modes are not identical. In Fig. 3(a) the gain is only sufficient for the two modes nearest the line center to break into oscillation. Consequently there is one component at  $c/2L$  and none at  $2(c/2L)$ . In Fig. 3(b) the gain is adequate for three modes to oscillate; there exist two discrete frequencies at  $c/2L$  and one at  $2(c/2L)$ . In Fig. 3(c) four modes are oscillating; there exist three different ways of obtaining the  $c/2L$  beat and two for the  $2(c/2L)$  beat. Finally, in Fig. 3(d) the gain is high enough for five modes to oscillate; there exist four ways of obtaining the 160-Mc/sec beat and three ways of obtaining the 320-Mc/sec beat. The expected components at frequencies higher than 320 Mc/sec have since been observed.<sup>10</sup>

There are two important consequences of the interpretation of the data in Fig. 3. The first is that one may deduce the number of even-symmetric modes which are oscillating from the beat splitting. The second is that in the case of three simultaneously oscillating modes [Fig. 3(b)] it seems probable that the frequency difference between the two  $c/2L$  components should increase with the difference in frequency between the central cavity resonance and the center of the Doppler line. Hence, for example, the two  $c/2L$  beats could be used to generate an error frequency (whose sharpness would be determined by the linewidth of the oscillation)<sup>2,11</sup> which could be used in a magnetostrictive tuning device to stabilize the central mode near the center of the Doppler line. The second consequence follows from a reasonably general symmetry argument. If we assume that the Doppler line shape is perfectly symmetric about its center frequency and that there are only three modes oscillating, any splitting in the  $c/2L$  beats must arise from an asymmetric distribution of the three modes about the Doppler center. That is, if the central cavity mode is

precisely on the Doppler center, the pulling on the other two resonances must be equal and opposite; hence in this case no splitting can occur.

#### 4. PARAMETERS IN THE PRESENT MASER

For convenience, we summarize the pertinent parameters characteristic of the present maser in this section.

The frequency separation of the cavity resonances ( $c/2L$ ) is nominally  $\cong 160$  Mc/sec (Table I). The wavelength of the maser transition is 11 522.76 Å and corresponds to the  $2s_2$  to  $2p_4$  line of neon in Paschen notation.<sup>3</sup> From direct gain measurements on this transition under similar discharge conditions, the fractional energy gain in a single pass through the interferometer should be about 6%. The known reflectance losses<sup>4</sup> ( $\cong 1\%$ ) imply a cavity width ( $\Delta\nu_c$ ) of about  $\frac{1}{2}$  Mc/sec [Eq. (3) below]. However, the data in Table I taken with the analysis below, demonstrate that  $\Delta\nu_c$  is closer to 1 Mc/sec and that the total energy loss per pass is about 2%. Hence the maximum gain available corresponds to about three times the threshold for oscillation. The latter is in good agreement with the maximum number of modes observed [Fig. 3(d)] and the 800-Mc/sec Doppler width assumed below.

In the limit of complete resonance trapping of vacuum ultraviolet photons, the effective decay rates of the upper and lower maser levels are about  $10^7$  sec<sup>-1</sup> and  $8 \times 10^7$  sec<sup>-1</sup>, respectively.<sup>12</sup> The exact value of the natural linewidth ( $\Delta\nu_n$ ) for the maser transition depends critically on the unknown, vacuum ultraviolet decay rate of the upper maser level. It is expected, however, that  $15 < \Delta\nu_n < 80$  Mc/sec (see Sec. 10).

The full Doppler width at half-maximum intensity for neon atoms at the temperature of the maser is about 800 Mc/sec. The inelastic collision with the He( $2^3S$ ) atom by which the excited neon state is formed<sup>1</sup> is, of course, exothermic by  $\cong 1.5kT$  at room temperature. However, since the He atom has  $\frac{1}{3}$  the mass of the neon atom, it will carry off most of the energy by which the reaction is exothermic. Although the Doppler width will increase with the gas temperature and hence with the power output in the maser, it does so as the square root of the absolute temperature. Hence a Doppler width much in excess of 800 Mc/sec is not to be expected. It is inconceivable, for example, that the Doppler width could increase sufficiently with power to explain the magnitude of the anomalous power dependence of the beat frequencies reported above.

#### 5. MODE PULLING ANALYSIS

We are only concerned with the dominant modes of even radial symmetry corresponding to longitudinal propagation in a plane parallel Fabry-Perot interferometer. In what follows it is assumed that steady-

<sup>10</sup> A. J. Rack (private communication).

<sup>11</sup> The linewidths implied by the data in Fig. 3 are limited by the resolution of the spectrum analyzer.

<sup>12</sup> W. R. Bennett, Jr., in *Advances in Quantum Electronics*, edited by J. R. Singer (Columbia University Press, New York, 1961), p. 28.

state oscillation has been obtained in the system and that no coupling effects exist between simultaneously oscillating modes through time-dependent nonlinearities in the medium. These assumptions are likely to break down at some point. However, what is sought are manageable, approximate solutions which will explain the dominant mode pulling effects.

The oscillation frequency in the maser is determined primarily by a condition on the phase of the electric field and the phase shifts of importance all arise from single-pass time delays. By definition, the phase shift resulting from a wave traveling once through an interferometer of length  $L$  at a phase velocity  $c/n$  (where  $n$  is the refractive index) is

$$\varphi = 2\pi\nu Ln/c. \quad (1)$$

For a standing wave to build up in the cavity, the single-pass phase shift must be an integral multiple of  $\pi$ . Hence the evacuated cavity ( $n=1$ ) has resonant frequencies which are separated by  $c/2L$ .

From Eq. (1), the dispersion  $(\partial\varphi_c/\partial\nu)$  for the evacuated cavity ( $n=1$ ) is a constant. It is convenient to express  $\partial\varphi_c/\partial\nu$  in terms of the fractional energy loss per pass  $f$  and the full width of the cavity resonance at half-maximum intensity,  $\Delta\nu_{0c}$ . To accomplish the latter, we visualize a situation in which energy ( $U$ ) is placed in the evacuated cavity in the mode of interest. This energy decays exponentially with time at the rate  $(c/L)f$ . As a result, the frequency response of the interferometer is not perfectly sharp and one may define a  $Q$  for the evacuated cavity given by

$$Q_{0c} = \frac{2\pi\nu_{0c}U}{(cf/L)U} = \frac{\nu_{0c}}{\Delta\nu_{0c}}. \quad (2)$$

From (1) and (2),

$$\partial\varphi_c/\partial\nu = 2\pi L/c = f/\Delta\nu_{0c} = \text{const} \cong 2 \times 10^{-8} \text{ rad-sec}. \quad (3)$$

For the present system, a single-pass loss of one percent corresponds to  $\Delta\nu_{0c} \cong (1/2)\text{Mc/sec}$ .

There will, in general, be some entirely negligible contribution to  $(\partial\varphi_c/\partial\nu)$  arising from the resonant nature of the mirror reflectance coefficient. For example, in the present case the mirror transmission loss varied by a factor of two over a total range of about 1000 Å (or  $2 \times 10^{12}$  cycles/sec). If one then estimates the dispersion at maximum reflectance using a Lorentzian line shape [Eq. (9)], it is seen that the contribution from the mirrors is about  $5 \times 10^{-15}$  rad-sec. Hence the inclusion of this term alters Eq. (3) by about 2 parts in  $10^7$ . The inclusion of this term in the analysis given below merely changes the final pulling term in Eq. (22) by the same fractional amount and has no important effect on the absolute frequency of the oscillation. We therefore ignore this contribution to  $(\partial\varphi_c/\partial\nu)$ .

The introduction of the amplifying medium changes the refractive index in the system, thereby altering the single-pass phase shift from that obtained in the

evacuated case. Oscillation therefore occurs at another frequency  $\bar{\nu}$ , differing from the cavity resonance frequency  $\nu_{0c}$ , such that the single-pass phase shift is still an integral multiple of  $\pi$ . Since the cavity dispersion is large compared to that for the amplifying medium, oscillation occurs close to  $\nu_{0c}$  and the pulling is small. It is convenient to formulate the problem in terms of the difference in frequency from the cavity resonance. In particular, the maser oscillates at that frequency  $\bar{\nu}$  such that

$$(\partial\varphi_c/\partial\nu)(\bar{\nu} - \nu_{0c}) + \Delta\Phi_m(\bar{\nu}) = 0. \quad (4)$$

Here,  $\Delta\Phi_m(\bar{\nu})$  is the total change in single-pass phase shift at the actual frequency of oscillation which is caused by the insertion of the medium.  $\Delta\Phi_m(\bar{\nu})$  is composed of two parts and, from Eq. (1), may be expressed as

$$\begin{aligned} \Delta\Phi_m(\bar{\nu}) &= (2\pi L/c)[(n_0-1) + (n-1)]\bar{\nu} \\ &\equiv (2\pi L/c)(n_0-1)\bar{\nu} + \Delta\varphi_m(\bar{\nu}). \end{aligned} \quad (5)$$

The first term in Eq. (5),  $(2\pi L/c)(n_0-1)\bar{\nu}$ , arises from the density of ground-state atoms in the maser and from the density of excited atoms which may participate in neighboring transitions (e.g., the  $2^3S-2^3P$  of He at 10 830 Å). That is, this first term arises from a refractive index which is essentially independent of the frequency over the range of interest. Its main source in the helium-neon maser is the He( $1S$ ) at 1 mm Hg for which  $(n_0-1) \cong 5 \times 10^{-8}$ .<sup>13</sup>

From Eqs. (3) and (5), Eq. (4) may be expressed,

$$\bar{\nu} = \left(\frac{\nu_{0c}}{n_0}\right) - \left(\frac{\Delta\nu_{0c}/n_0}{f}\right)\Delta\varphi_m(\bar{\nu}).$$

We include the effects of  $n_0$  by defining

$$\bar{\nu}_c = \nu_{0c}/n_0 \quad \text{and} \quad \Delta\nu_c = \Delta\nu_{0c}/n_0. \quad (6)$$

Hence the oscillator frequency ( $\bar{\nu}$ ) is given by

$$\bar{\nu} = \bar{\nu}_c - (\Delta\nu_c/f)\Delta\varphi_m(\bar{\nu}). \quad (7)$$

For the helium-neon case,  $\Delta\nu_c$  in Eq. (6) differs negligibly ( $\cong 5$  parts in  $10^8$ ) from  $\Delta\nu_{0c}$  in Eq. (3). Similarly, the frequency separation between adjacent cavity resonances differs by the same negligible constant amount from  $c/2L$ . For an arbitrary setting of the interferometer,  $n_0$  does introduce a pressure-dependent shift in the oscillator frequency of about 13 Mc/sec per mm Hg of He. However, in the special case that  $\nu_c$  is tuned to the center of a symmetric line (see below), the oscillator frequency is independent of  $\nu_c$  and this pressure-dependent shift vanishes.

The term  $\Delta\varphi_m(\bar{\nu})$  in Eqs. (5) and (7) is a function of the fractional energy gain per pass  $g(\bar{\nu})$ . Since the latter varies with frequency over the transition responsible for the amplification  $\Delta\varphi_m$  does also. Generally,  $\Delta\varphi_m$  goes through zero at the line center ( $\nu_m$ ), is negative

<sup>13</sup> *American Institute of Physics Handbook* (McGraw-Hill Book Company, Inc., New York, 1957), pp. 6-21.

("anomalous dispersion") for frequencies less than  $\nu_m$ , and is positive for frequencies greater than  $\nu_m$ . Equation (6) therefore predicts a shift in the direction of the line center.

Threshold for oscillation occurs at that frequency  $\bar{\nu}_T$ , satisfying both Eq. (7) and the condition  $g(\bar{\nu}_T) = f$ . The latter generally results in a transcendental equation for  $\bar{\nu}_T$ . In the special case of a Lorentzian line, the transcendental nature of this equation is removed.

The existence of a steady-state oscillation above threshold obviously implies that the gain at the frequency of oscillation must saturate at

$$g(\bar{\nu}) = f. \quad (8)$$

In the case of homogeneous or "natural" broadening, gain proportionality is always maintained over the line. That is, the reduction of the gain at frequency  $\bar{\nu}$  necessary to satisfy Eq. (8) produces a proportionate reduction of the gain at all other frequencies. Hence in the case of homogeneous broadening, the oscillation frequency is always given by its value at threshold and there is no direct power-dependent pulling effect. In the case of inhomogeneous broadening (applying to the He-Ne maser), the interpretation of requirement (8) is more complicated.

## 6. ASSUMPTIONS ON LINE SHAPE

In general,  $\Delta\varphi_m$  will be a function of the single-pass gain and for a given line shape could be calculated numerically from the Kramers-Kronig relations.<sup>14</sup>

For a Lorentzian line, it may be shown (see Appendix I) that

$$\Delta\varphi_m(\nu) \cong -\frac{g_m(\nu_m - \nu)}{\Delta\nu_m} \left[ 1 + \frac{4(\nu_m - \nu)^2}{(\Delta\nu_m)^2} \right]^{-1}, \quad (9)$$

where the fractional energy gain per pass at the frequency  $\nu$  is given by

$$g(\nu) \cong g_m \left[ 1 + 4(\nu_m - \nu)^2 / (\Delta\nu_m)^2 \right]^{-1}. \quad (10)$$

Here, as in the rest of this paper, we adopt the notation that  $g_m$  is the fractional energy gain per pass at the line center ( $\nu_m$ ), and that  $\Delta\nu_m$  is the full width of the line at half-maximum fractional energy gain. The approximations in (9) and (10) arise from the assumption that  $\nu + \nu_m = 2\nu$  and that  $g_m \ll 1$ . Equations (9) and (10) may be expressed

$$\Delta\varphi_m(\nu) \cong -g(\nu)(\nu_m - \nu) / \Delta\nu_m. \quad (11)$$

The Lorentzian form will be used in this paper to obtain an accurate expression for the pulling in the case of natural broadening and to allow for the holes produced by inhomogeneous broadening in the case of the helium-neon maser.

<sup>14</sup> D. E. Thomas (to be published) has extended his "Tables of Phase of a Semi-Infinite Unit Attenuation Slope" (Bell System Monograph 2550) to handle general problems of the present type numerically. His results for the special case of a Gaussian have been verified analytically by A. Javan.

What actually is involved in the helium-neon maser is a Gaussian distribution of Lorentzian lines resulting from the thermal motion of the excited neon atoms and the corresponding Doppler shift of the atoms' center frequencies. Hence, in the limit (holding here) that the natural linewidth is small compared to the Doppler width, the line much more closely resembles a Gaussian than a Lorentzian.

We are primarily concerned with effects taking place within the full width of the line at half-maximum intensity and in the limit of small energy gain. In the limit of small gain, it is apparent from the Kramers-Kronig relations<sup>15</sup> that the phase shift increases linearly with the gain. Hence for any typical symmetric line, the phase shift introduced by the amplifying medium may be expanded in the series

$$\Delta\varphi_m(\nu) \cong -ag_m \left( \frac{\nu_m - \nu}{\Delta\nu_m} \right) \left[ 1 - b \left( \frac{\nu_m - \nu}{\Delta\nu_m} \right)^2 + \dots \right], \quad (12)$$

where the constants  $a$  and  $b$  will depend on the lineshape. Since  $\Delta\varphi_m$  must have odd symmetry about the line center, approximation (12) involves the assumption that  $[(\nu_m - \nu) / \Delta\nu_m]^4 \ll 1$ . Hence, approximation (12) will be extremely good over a considerable range within the central portion of the line and will fail rapidly for frequencies occurring near the half-intensity points on the gain curve. Approximation (12), of course, consists of the first two terms in the expansion of the sine function and for manipulative reasons it is convenient to express  $\Delta\varphi_m$  in the latter way. In particular, a "best fit" of numerical calculations<sup>14</sup> made by Thomas<sup>14</sup> demonstrates that

$$\Delta\varphi_m(\nu) \cong -0.28_2 g_m \sin \left( \frac{\nu_m - \nu}{0.3\Delta\nu_m} \right) \quad (13)$$

is an exceptionally good approximation for a Gaussian. Both "angles" in Eq. (13) are expressed in radians. The errors introduced by a literal interpretation of (13) are less than 1% for  $|\nu_m - \nu| \leq 0.4\Delta\nu_m$ . Equation (13) is  $\cong 6\%$  low at the half-intensity points on the curve. For  $|\nu_m - \nu| > 0.5\Delta\nu_m$  the error increases exponentially. The corresponding fractional energy gain for the Gaussian is,

$$g(\nu) \cong g_m \exp \left[ - \left( \frac{\nu_m - \nu}{0.6\Delta\nu_m} \right)^2 \right]. \quad (14)$$

From (13) and (14)

$$\Delta\varphi_m(\nu) \cong -0.28_2 g(\nu) \exp \left[ \left( \frac{\nu_m - \nu}{0.6\Delta\nu_m} \right)^2 \right] \sin \left( \frac{\nu_m - \nu}{0.3\Delta\nu_m} \right) \quad (15)$$

holds for a Gaussian within the central region of the curve.

<sup>15</sup> See, for example, J. H. Van Vleck, *Radiation Laboratory Series* (McGraw-Hill Book Company, Inc., New York, 1948), Vol. 13, Chap. 8.

### 7. HOMOGENEOUS BROADENING

For a homogeneously broadened Lorentzian line, (7), (8), and (11) yield

$$\bar{\nu} = (\nu_c \Delta \nu_m + \nu_m \Delta \nu_c) / (\Delta \nu_m + \Delta \nu_c) \quad (16)$$

for the oscillation frequency where definition (6) is assumed.<sup>16</sup> In the limit that  $\Delta \nu_c < \Delta \nu_m$ , (16) becomes

$$\bar{\nu} = \nu_c + (\nu_m - \nu_c) \left( \frac{\Delta \nu_c}{\Delta \nu_m} \right) \left[ 1 - \frac{\Delta \nu_c}{\Delta \nu_m} + \dots \right], \quad (17)$$

and in the Lorentzian case, the pulling is linearly dependent on the frequencies. The latter would, of course, not be true in the case of an inhomogeneously broadened Lorentzian line above threshold. As may be seen by comparing the expanded terms of Eqs. (9) and (13), the phase characteristic of the Lorentzian is actually about twice as nonlinear as that of the Gaussian near the line center.

For a Gaussian line, (7), (8), and (15) yield,

$$\bar{\nu} = \nu_c + 0.28_2 \Delta \nu_c \exp \left[ \left( \frac{\nu_m - \bar{\nu}}{0.6 \Delta \nu_m} \right)^2 \right] \sin \left( \frac{\nu_m - \bar{\nu}}{0.3 \Delta \nu_m} \right), \quad (18)$$

and the pulling is nonlinear even in the homogeneously broadened case. For frequencies very near the line center in the limit that  $\Delta \nu_c < \Delta \nu_m$ , Eq. (18) becomes

$$\bar{\nu} = \nu_c + (\nu_m - \nu_c) (0.94 \Delta \nu_c / \Delta \nu_m) \times [1 - 0.94 (\Delta \nu_c / \Delta \nu_m) + \dots]. \quad (19)$$

Hence, for frequencies near the center of the line in the limit  $\Delta \nu_c \ll \Delta \nu_m$ , the main difference between the Gaussian and the Lorentzian is a 6% reduction in the pulling factor.

Equation (18) only applies to the helium-neon maser in the case of threshold for the first cavity resonance. For an inhomogeneously broadened line, an expansion of the threshold pulling term in powers of  $\Delta \nu_c / \Delta \nu_m$  is misleading. The neglected nonlinear terms are generally much larger than  $(\Delta \nu_c / \Delta \nu_m)^2$ . The latter is apparent for Eq. (18), but is also true of Eq. (16). The inhomogeneously broadened case may be more realistically treated through the method given below.

### 8. GENERAL APPROXIMATE SOLUTION FOR OPTICAL MASERS

Generally for optical masers,  $\Delta \nu_m \gg \Delta \nu_c$  and  $\Delta \varphi_m(\nu)$  will be a slowly varying function of the frequency over the cavity resonance. We may therefore expand  $\Delta \varphi_m$  in a Taylor series about the cavity resonance frequency, obtaining

$$\Delta \varphi_m = (\Delta \varphi_m)_{\nu_c} + (\partial \Delta \varphi_m / \partial \nu)_{\nu_c} (\nu - \nu_c) + \dots \quad (20)$$

<sup>16</sup> Equation (16) is equivalent to a result quoted by C. H. Townes, in *Advances in Quantum Electronics*, edited by J. R. Singer (Columbia University Press, New York, 1961), p. 10.

Substituting Eq. (20) in Eq. (7) yields

$$\bar{\nu} = \nu_c - (\Delta \nu_c / f) \Delta \varphi_m(\nu_c) \times [1 - (\Delta \nu_c / f) (\partial \Delta \varphi_m / \partial \nu)_{\nu_c} + \dots]. \quad (21)$$

As may be seen by comparison with Eqs. (17) and (19), this last approximation is equivalent to an expansion of the pulling terms in powers of  $(\Delta \nu_c / \Delta \nu_m)$  which still retains the nonlinear properties of the phase characteristic. Typically,  $(\Delta \nu_c / \Delta \nu_m) \cong 10^{-3}$ . Hence the oscillator frequency is given by

$$\bar{\nu} \cong \nu_c - (\Delta \nu_c / f) \Delta \varphi_m(\nu_c), \quad (22)$$

where errors in the second term of about a part in  $10^3$  (i.e., about 200 cycles/sec in the absolute frequency for the helium-neon maser) may be expected.  $\Delta \varphi_m(\nu_c)$  represents the actual phase shift introduced by the amplifying transition at the cavity resonance in the presence of oscillation. Equation (22) may be solved numerically using the methods of Thomas<sup>14</sup> in the general case (e.g., asymmetric lines) for both homogeneous and inhomogeneous broadening.

### 9. EFFECT OF HOLES

It is in the interpretation of requirement (8) that an important difference arises between the helium-neon maser and, for example, the ammonia maser (or more generally, between the present oscillator and most other oscillators). In the present system, the line is primarily broadened by the Doppler effect. Consequently, reduction of the gain at the frequency  $\bar{\nu}$  in order to satisfy Eq. (8) does not imply a proportionate reduction of the gain at other frequencies. If the converse were true (as in the case of homogeneous broadening), a second cavity mode would generally not go into oscillation; i.e., the saturation requirement (8) at the first resonance would prevent the second cavity resonance from reaching threshold. In the present case, (8) is satisfied by burning a hole in the line.  $g(\bar{\nu})$  saturates at  $f$ , whereas the gain over the rest of the line continues to increase with pumping rate. In other words, the phase shift introduced at the cavity resonance continues to increase as the number of upper state atoms increases at frequencies well removed from the hole. We shall satisfy requirement (8) in the following analysis by subtracting the phase shift which would have been produced by atoms in the hole from the phase shift introduced by the entire distribution in the absence of oscillation. In evaluating these phase shifts, we make use of the same approximation implicit in Eq. (22)—namely, that  $\bar{\nu}$  may be replaced by  $\nu_c$ .

Before taking explicit account of the holes, we make the following two observations:

(a) Since atoms on opposite sides of the cavity resonance ( $\nu_c$ ) contribute to the gain at  $\nu_c$  with the same sign, the total gain at  $\nu_c$  is determined primarily by those atoms whose center frequencies fall within the resonance by about one natural linewidth. Hence,

variations in the upper state density at large frequency separations from the cavity resonance do not affect the gain at  $\nu_e$  appreciably, and a hole burned at one resonance does not have an important first-order effect on the gain at another resonance.

(b) Since atoms on opposing sides of the cavity resonance contribute to the phase shift at  $\nu_e$  with opposite sign, the net phase shift at  $\nu_e$  is determined primarily by atoms which are well removed from the cavity resonance. Hence the absence of atoms (i.e., a hole) at one resonance can have a large first-order effect on the phase shift at another resonance. The presence of a hole at one resonance reduces the pulling at another resonance which would have existed in the absence of the hole. That is, two holes always tend to repel each other. However, since a hole represents a symmetric removal of atoms about a cavity resonance to first order, a hole does not have a first-order effect on itself.

It is shown in Appendix II that the probability for stimulated emission is a Lorentzian function of the frequency separation between the mode of oscillation and the center frequency of the atoms involved. In addition, it is shown that the full width at half-maximum for this probability distribution is a function of the power in the mode and, hence, of the gain at the resonance. We therefore assume that the holes burned in the line will be Lorentzian in shape and have widths dependent on their location in respect to the line center. Although the Lorentzian hole shape would only hold strictly for a constant distribution of atoms, it is apparent that it will represent a good first-order approximation at low powers in the present case.

By analogy with Eq. (9), the phase shift introduced at frequency  $\nu_2$  by a Lorentzian hole centered at frequency  $\nu_1$ , is

$$\Delta\varphi_H(\nu_2) = \frac{D_1(\nu_1 - \nu_2)}{H_1} \left[ 1 + \frac{4(\nu_1 - \nu_2)^2}{H_1^2} \right]^{-1}, \quad (23)$$

where  $D_1$  is the depth of the hole at  $\nu_1$  and  $H_1$  is the full width of this hole at half-maximum intensity. The sign on Eq. (23) is opposite to that for Eq. (9) since we are concerned with phase shifts introduced by the absence of atoms. Since we are only interested in the phase shift produced at one resonance by holes at different resonances [observation (b) above],  $|\nu_1 - \nu_2| \geq (c/2L)$ . In the low power limit, we may assume that the hole widths are less than the hole separations and consequently that  $4(\nu_1 - \nu_2)^2 \gg H_1^2$ . This approximation introduces an error of about 5% in the evaluation of  $\Delta\varphi_H$  for the hole widths required below to explain the anomalous increase in beat frequency with pumping rate. Therefore,

$$\Delta\varphi_H(\nu_2) \cong \left( \frac{g(1) - f}{4} \right) \left( \frac{H_1}{\nu_1 - \nu_2} \right), \quad (24)$$

where we have defined  $D_1 = g(1) - f$  in conformance

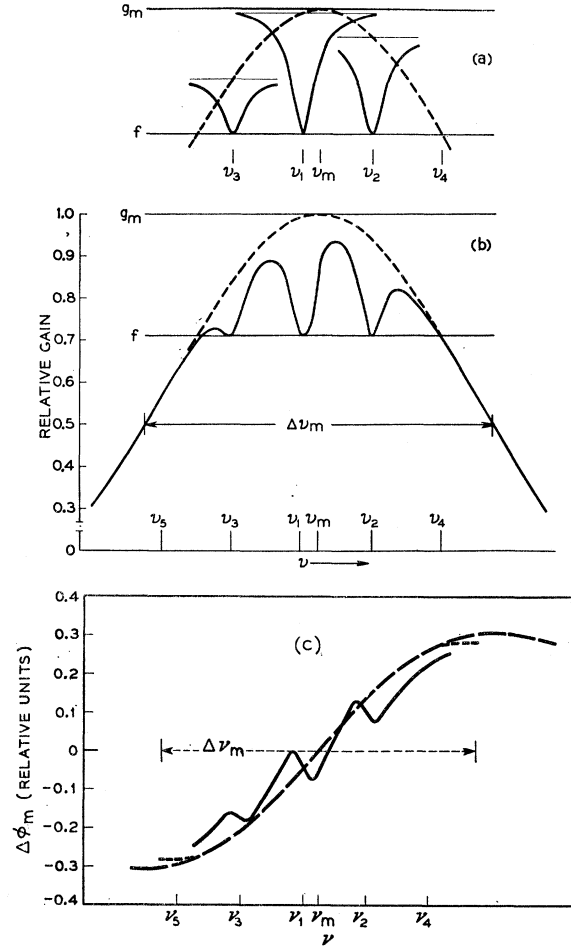


FIG. 4. "a" illustrates the choice of hole depth used to satisfy Eq. (8). "b" illustrates the resultant line shape at threshold for the fourth cavity resonance when  $\nu_m - \nu_1 = 40$  Mc/sec.  $\Delta\nu_m = 800$  Mc/sec and  $c/2L = 160$  Mc/sec. Equal hole widths of 64 Mc/sec have arbitrarily been assumed. "c" (the solid curve) illustrates the resultant variation of the total phase shift for the condition in "b". The dashed curve represents the phase shift introduced by the original Gaussian. The dotted curve shows the departure of approximation (13) from the actual phase characteristic of the Gaussian.

with saturation condition (8). This choice of hole depth is illustrated in Fig. 4(a) for the case of three resonances.

The total phase shift introduced at frequency  $\nu_j$  by  $N$  Lorentzian holes at frequencies  $\nu_i$  is then

$$\Delta\varphi_H(j) \cong \sum_{i=1, (i \neq j)}^N \left( \frac{g(i) - f}{4} \right) \left( \frac{H_i}{\nu_i - \nu_j} \right). \quad (25)$$

From Eqs. (22) and (25) the oscillation frequency for the  $j$ th cavity resonance is given by

$$\bar{\nu}_j \cong \nu_j - \frac{\Delta\nu_e}{f} \Delta\varphi_m(\nu_j) - \frac{\Delta\nu_e}{4} \sum_{i=1, (i \neq j)}^N \left( \frac{g(i)}{f} - 1 \right) \left( \frac{H_i}{\nu_i - \nu_j} \right), \quad (26)$$

where by definition  $g(i) \geq f$  for a hole to occur at frequency  $\nu_i$ . The quantities  $g(i)$  are related by Eq. (14) and  $\Delta\varphi_m$  is given by Eq. (13) for a Gaussian line. For a Lorentzian line, Eqs. (9) and (10) obtain.

A numerical evaluation of the total phase shift over the central portion of a Gaussian line is illustrated in Fig. 4(c) for three Lorentzian lines. The errors introduced by approximation (13) are also indicated in Fig. 4(c).

#### 10. HOLE WIDTHS FROM STIMULATED EMISSION

From Eq. (II.11) of Appendix II, the full width ( $H$ ) of a hole produced by stimulated emission is

$$H = \left( \frac{\gamma_a + \gamma_b}{2\pi} \right) \left( 1 + \frac{1}{\gamma_a \gamma_b} \left| \frac{2V}{\hbar} \right|^2 \right)^{\frac{1}{2}}, \quad (27)$$

$\gamma_a$  and  $\gamma_b$  represent the decay rates of the upper and lower maser levels, respectively, and the matrix element  $V$  is given by

$$|V|^2 = |eE_0(z)_{a,b}/2|^2, \quad (28)$$

where  $E_0$  is the amplitude of the electric field in the cavity mode.  $E_0^2$  is proportional to the power ( $P$ ) expended in the mode and may be readily expressed the latter way through the known cavity  $Q$  and volume ( $v = 108 \text{ cm}^3$ ) of the discharge;

$$E_0^2 = 4P/(v\Delta\nu_c). \quad (29)$$

The upper maser level may decay by several transitions, hence

$$\gamma_a = \gamma_{ab} + \gamma_{ac} + \dots, \quad (30)$$

where

$$\gamma_{ab} = \frac{4}{3} \frac{e^2}{\hbar\lambda^3} |r_{ab}|^2 \cong \frac{4e^2}{\hbar\lambda^3} |z_{ab}|^2, \quad (31)$$

where  $\lambda$  and  $\hbar$  are, respectively, the wavelength for the transition and Planck's constant divided by  $2\pi$ . Combining Eqs. (27), (28), (29), and (31) yields

$$H \cong \frac{\gamma_a + \gamma_b}{2\pi} \left( 1 + \frac{\gamma_{ab}}{\gamma_a \gamma_b} \frac{\lambda^3 P}{\hbar v \Delta\nu_c} \right)^{\frac{1}{2}}, \quad (32)$$

where cgs units are used and the coefficient outside the square root,

$$\Delta\nu_n = (\gamma_a + \gamma_b)/2\pi, \quad (33)$$

represents the natural linewidth for the transition.

If the decay rates in Eq. (32) were determined entirely by known spontaneous radiative values, the interpretation of Eq. (32) would be straightforward. The effective decay rates for the two maser levels have approximate values<sup>12</sup> of

$$\begin{aligned} \gamma_a &\cong 10^7 \text{ sec}^{-1}, \\ \gamma_b &\cong 8 \times 10^7 \text{ sec}^{-1}. \end{aligned} \quad (34)$$

However, the vacuum ultraviolet portion of the decay rate of the upper maser level is unknown. The resonance trapping process [which determines the effective, long lifetime of the upper maser level given in Eq. (34)] will interrupt the phase of the wave function used to obtain Eq. (27) by some unknown, large extent. Consequently, an unambiguous interpretation of Eq. (32) cannot be given and we may only examine two limiting cases. The first limit is obtained by inserting the values (34) in Eq. (32). Here one obtains the minimum hole width (15 Mc/sec) at threshold and the maximum dependence of the hole width on power. From the measured power in the beam and estimates of the other parameters involved, the hole widths in this limiting case might extend to about 50 Mc/sec at the highest output powers obtained. The second limit is obtained through the marginal observation of a clean  $c/2L$  beat at low powers in another He-Ne maser having twice the length of the present one. This observation implies that the natural linewidth for the transition is less than 80 Mc/sec. Hence in the second limiting case maximum hole widths of about 100 Mc/sec might be obtained at high powers from stimulated emission.

A related point of interest arises here which should be noted. Namely, because of the phase-interruption process, more output power is to be expected from a maser transition in which the upper state is optically connected with the ground state than for one which is not. That is, the hole widths in the former case will be larger, even if the effective decay rates and oscillator strengths for the two maser transitions are identical.

#### 11. EFFECTS OF ELASTIC SCATTERING

There exist only two likely sources by which the upper state atoms may migrate over the Doppler distribution during their lifetimes:

- (1) large-angle elastic scattering,
- (2) small-angle elastic scattering.

We have separated the elastic (atom-atom) scattering process into these two groups both because the nature of the differential scattering cross section readily permits this separation and because the effects of the two processes are in opposite directions.

Process (1) results in violent changes in velocity of the upper state maser atoms and, hence, in changes in the location of the atoms' center frequencies which are comparable to the full width of the Doppler line. This effect therefore tends to restore the gain proportionality condition which holds, for example, over the entire line in the case of natural broadening. Thus, process (1) tends to oppose the burning of holes in the line. Its effects, however, are small in the present case. The total large-angle scattering cross-section for atoms in the upper neon maser state on ground state He atoms is unknown. However the known<sup>17</sup> diffusion rates of the

<sup>17</sup> A. V. Phelps and J. P. Molnar, Phys. Rev. **89**, 1202 (1953).

metastable He( $2^3S_1$ ) and Ne( $3^3P_2$ ) levels in their own gases both correspond to total ("hard sphere") large-angle scattering cross sections of about  $10^{-15}$  cm<sup>2</sup> at a pressure of 1 mm Hg, and a temperature of 300°K. Since the upper Ne maser level has a similar configuration ( $4^1P_1$  is *LS* notation) to the Ne( $3^3P_2$ ), it seems unlikely that the total large-angle elastic scattering cross section would be appreciably different in the present case. Hence we expect the total large-angle collision rate for the upper maser level for the pressures in the maser (1 mm Hg of He and 0.1 mm Hg of Ne) to be about  $0.5 \times 10^7$  sec<sup>-1</sup>. The latter corresponds to about half the known<sup>12</sup> decay rate of the upper maser level.

Process (1) therefore takes place  $\cong 0.5$  times per atom on the average and the probability of the atom landing in a hole at low powers may be neglected.

The small-angle collisions, however, will result in the widening of a hole burned in the line. In the real case, the tail of the Van der Waals interaction, the possibility of molecular bonds, etc., will increase the differential scattering cross section enormously at small angles. The magnitudes of these interactions are unknown in the present case. However, one may estimate the size of the effect by assuming a hard-sphere cross section corresponding to typical diffusion rates. From the quantum mechanical treatment of the hard-sphere problem,<sup>18</sup> there is always a cone of small, finite half-angle,

$$\theta \cong h/2\mu_m v_{rel} a, \quad (35)$$

within which the scattering is nonclassical and within which the total scattering rate is generally about equal to the total large-angle scattering rate. Here,  $\theta$  is given in the center of mass system,  $\mu_m$  is the reduced mass,  $v_{rel}$  the relative velocity,  $h$  is Planck's constant, and  $a$  is the molecular diameter. This type of effect is difficult to observe experimentally and would not be included, for example, in the elastic scattering cross section measured in a diffusion experiment. We next assume that the average small-angle scattering event corresponds to scattering in the center-of-mass system through an angle  $\theta/2$ . This average small-angle collision between the excited neon atom and a ground-state helium atom therefore causes the excited neon atom to change its center frequency by an amount,

$$\delta\nu = \delta v_{Ne} \nu / c = \delta v_{rel} \nu / 6c \cong h\nu / 24\mu_m c a. \quad (36)$$

We next choose " $a$ " to correspond to the classical hard-sphere scattering cross section determined from the diffusion data in reference 17 (i.e.,  $\pi a^2 = 10^{-15}$  cm<sup>2</sup>) and obtain the result

$$\delta\nu \cong 30 \text{ Mc/sec.} \quad (37)$$

That is, the typical step is about equal to 30 Mc/sec and on the average half the atoms will make one such step in their lifetimes. Hence holes burned in the

Doppler line might be enlarged by  $\cong 15$  Mc/sec due to small-angle scattering.

## 12. SEMI-EMPIRICAL REPRESENTATION OF HOLE WIDTHS

From the discussion in Secs. 10 and 11, the hole widths at low powers will approach an unknown constant value falling in the tens of Mc/sec range. From the discussion in Sec. 10, it is apparent that well above threshold the hole widths will increase as the square root of the power in the mode. The power in the mode itself will be approximately proportional to the product of the hole width and the hole depth. Hence at high powers one expects

$$H_i \cong H_0 [g(i) - f] / f,$$

where the constant  $H_0$  will also be in the tens of Mc/sec range. Hence we may represent the width of the  $i$ th hole by

$$H_i \cong h_0 + H_0 [g(i) - f] / f \quad (38)$$

over the entire range in power. The adoption of Eq. (38) permits the evaluation of Eq. (26) with a minimum number of adjustable parameters.

## 13. COMPARISON OF MODE PULLING ANALYSIS WITH EXPERIMENT

Since the distribution of atoms is peaked at frequency  $\nu_m$ , there will be a definite order of appearance of the various possible cavity resonances. We shall enumerate these cavity resonance frequencies in order of their appearance:

$$\nu_1, \nu_2, \nu_3, \dots, \text{ where } \dots \nu_3 < \nu_1 < \nu_m < \nu_2 \dots \quad (39)$$

Condition (39) corresponds to the one illustrated in Fig. 4 and will be assumed below in the cases for which Eq. (26) is evaluated. In making the present comparisons we consider only the Gaussian line for which Eqs. (13), (14), and (15) apply.

Evaluation of Eq. (26) for the first two resonances ( $\nu_2 > \nu_1$ ) yields

$$\begin{aligned} \bar{\nu}_2 - \bar{\nu}_1 \cong & \left( \frac{c}{2L} \right) + \frac{\Delta\nu_c}{4(c/2L)} \left[ \left( \frac{g_1 - f}{f} \right) H_1 + \left( \frac{g_2 - f}{f} \right) H_2 \right] \\ & - 0.56 \frac{gm}{f} \Delta\nu_c \sin \left( \frac{c/2L}{0.6\Delta\nu_m} \right) \cos \left( \frac{\nu_m - \nu_1 - c/4L}{0.3\Delta\nu_m} \right), \quad (40) \end{aligned}$$

where  $g(1)$ ,  $g(2)$ , and  $g_m$  are related through Eq. (14) and it is assumed that  $g(2) \cong f > g(3)$ .

The first case of interest corresponds to threshold for the appearance of the  $c/2L$  beat and, therefore, the data in Table I. Here, Eq. (40) reduces to

$$\bar{\nu}_2 - \bar{\nu}_1 \cong (c/2L) [1 - 0.94(\Delta\nu_c/\Delta\nu_m)] \quad (41)$$

plus terms of order  $\Delta\nu_c(c/2L\Delta\nu_m)^3$ . The latter amount to frequency fluctuations in the order of 10 kc/sec and are within the limits of error quoted in Table I. Comparison

<sup>18</sup> N. F. Mott and H. S. W. Massey, *The Theory of Atomic Collisions* (Clarendon Press, Oxford, England, 1949), 2nd ed., Chap. II.

of Eq. (41) with the data in Table I implies that  $\Delta\nu_c \cong 1$  Mc/sec, since  $\Delta\nu_m \cong 800$  Mc/sec. This value of  $\Delta\nu_c$  is in discrepancy with the value ( $\cong 0.5$  Mc/sec) obtained from Eq. (3) for the known (0.99) mirror reflectance coefficient and suggests that some additional loss of about 1% per pass is present in the maser other than that introduced by the mirror reflectance coefficient. Fox and Li<sup>19</sup> have made tentative estimates which indicate that a loss of this approximate magnitude might arise from mode mixing at the end plates from flatness irregularities. In support of this contention we note that the present maser obviously has more loss than the first one reported<sup>1</sup> since it oscillated only on the strongest of the five transitions of neon previously observed. Here the main difference between the two masers is that the first maser had Fabry-Perot plates of considerably higher quality. It is conceivable that the reflectance films in the present maser deteriorated by the required amount during bakeout,<sup>8</sup> in which case the contention is not clearly established. It was found, however, that the loss implied by the data in Table I remained constant within the limits of error quoted over six months of continuous operation. In what follows, we assume that the ratio  $\Delta\nu_c/\Delta\nu_m \cong 1/800$  has been experimentally determined from the data in Table I.

The second term in Eq. (40) increases with the power and consequently is capable of explaining the anomalous behavior of the  $c/2L$  beat reported in Sec. 3. The hole repulsion effect, however, can only explain this anomalous behavior if it dominates over the third term in Eq. (40). The variation of the beat frequency above threshold will obviously be a complicated function of the location of  $\nu_1$  in respect to the line center. There are two extreme limiting cases and we only consider these. Because of the large number of exponential terms, it is simplest to solve Eq. (40) numerically. The results quoted below are for the parameters characteristic of the present maser—namely  $c/2L \cong 160$  Mc/sec,  $\Delta\nu_m \cong 800$  Mc/sec, and  $\Delta\nu_c \cong 1$  Mc/sec. In evaluating Eq. (40) we express the total excursion of the beat between threshold for its appearance and threshold for the next cavity resonance. Hence, through the use of Eqs. (14) and (38), only two adjustable parameters  $h_0$  and  $H_0$  appear in the final result.

The first limiting case corresponds to a symmetric placement of the two cavity resonances about the Doppler line. Here the minimum hole repulsion effect should occur since both resonances cross threshold simultaneously and the two hole widths must be the same minimum value at threshold. A numerical solution of Eqs. (14), (38), and (40) for the present maser in this limiting case yields

$$(\bar{\nu}_2 - \bar{\nu}_1)_{\max} - (\bar{\nu}_2 - \bar{\nu}_1)_{\text{thresh}} \cong 0.75[h_0 + 0.25H_0 - 60] \text{ kc/sec,} \quad (42)$$

where the bracketed quantities are expressed in Mc/sec.

<sup>19</sup> A. G. Fox and Tingye Li (private communication).

The fact that an interferometer setting could be found (Sec. 3) for which the  $c/2L$  beat was nearly independent of power suggests that the bracketed quantity in Eq. (42) is very close to zero. Hence we expect

$$h_0 + 0.25H_0 \cong 60 \text{ Mc/sec} \quad (43)$$

for the present maser.

The other limiting case occurs at  $\nu_1 = \nu_m$ . Here the first hole may be enlarged considerably through stimulated emission before the second resonance occurs and the maximum hole repulsion effect should arise. This limit is complicated in the real case by the fact that both the second and third cavity resonances cross threshold simultaneously. Here the two  $c/2L$  beats are identical and splitting (see below) does not occur until the fourth and fifth cavity resonances cross threshold. The effect of the third hole will not alter the present estimate substantially, however, and we shall ignore its presence (i.e., the effects of the holes at  $\nu_2$  and  $\nu_3$  cancel at  $\nu_1$ , whereas the effects of the holes at  $\nu_1$  and  $\nu_3$  are additive at  $\nu_2$ ). A numerical evaluation of Eqs. (14), (38), and (40) in this limiting case ( $\nu_1 = \nu_m$ ) yields

$$(\bar{\nu}_2 - \bar{\nu}_1)_{\max} - (\bar{\nu}_2 - \bar{\nu}_1)_{\text{thresh}} \cong 1.3[h_0 + 0.55H_0 - 60] \text{ kc/sec} \quad (44)$$

for the parameters in the present maser. The bracketed quantities are again given in Mc/sec. If we assert that the extreme 30 kc/sec shift of the beat reported in Sec. 3 occurs in the second limiting case, Eqs. (43) and (44) imply that  $h_0 \cong 40$  Mc/sec and  $H_0 \cong 80$  Mc/sec. These values obviously do not represent precise measurements. However, they are sufficiently close to the estimates given in Secs. 10 and 11 to indicate that the hole repulsion effect is the correct explanation for the anomalous power dependence of the beat reported in Sec. 3.

Finally, it is important to note that Eq. (26) also predicts a splitting of the  $c/2L$  beat which is compatible with the magnitudes observed. Evaluation of Eq. (26) for three asymmetrically placed holes yields

$$(\bar{\nu}_2 - \bar{\nu}_1) - (\bar{\nu}_1 - \bar{\nu}_3) \cong \frac{3}{8} \frac{\Delta\nu_c}{(c/2L)} \left[ \left( \frac{g_2 - f}{f} \right) H_2 - \left( \frac{g_3 - f}{f} \right) H_3 \right] - 1.13 \Delta\nu_c \left( \frac{g_m}{f} \right) \left[ \sin \left( \frac{c/2L}{0.6\Delta\nu_m} \right) \right]^2 \sin \left( \frac{\nu_m - \nu_1}{0.3\Delta\nu_m} \right), \quad (45)$$

where no terms contained in Eqs. (13) and (26) have been neglected.  $g_2$  and  $H_2$  are the fractional energy gain and hole width at  $\nu_2$ , respectively;  $g_3$  and  $H_3$  are similarly defined at  $\nu_3$ ; and  $g_m$  is the fractional energy gain per pass at the line center. Equation (45) holds only for the case where  $g_3 \geq f$  and the gain at the fourth cavity resonance is below threshold for oscillation. Equation (45) predicts that the beat splitting will vanish for  $\nu_m = \nu_1$ , since in this case  $g_2 = g_3$  and  $H_2 = H_3$ .

In spite of its formidable appearance, Eq. (45) is a fairly linear function of  $(\nu_m - \nu_1)$ . The main nonlinear term arises from the power dependent part of the hole width in Eq. (38) and enters Eq. (45) as the difference between the squares of two small quantities. For the same reason, Eq. (45) is not strongly dependent on the parameter  $H_0$  at low powers. The splitting is primarily determined by the last term of Eq. (45). Its maximum value occurs at  $\nu_m - \nu_1 = \frac{1}{2}(c/2L)$  and at a value for  $g_m$  such that the fourth cavity resonance is just below threshold. For the present maser, the maximum value of the second term is a little over 50 kc/sec and hence somewhat in excess of the maximum splitting ( $\cong 30$  kc/sec) observed. By definition [Eqs. (38) and (39)], the first term in Eq. (45) is positive and, hence subtracts from the nonlinear phase characteristic of the Gaussian. At low powers this subtracted term is mainly determined by the width,  $h_0$  in Eq. (38). For the present maser, the inclusion of  $h_0$  in Eq. (45) would reduce the maximum splitting by about 0.5 kc/sec per Mc/sec of  $h_0$ . Hence for the value of  $h_0$  estimated above ( $\cong 40$  Mc/sec), the first term of Eq. (45) would reduce the maximum splitting from the second term to about that value observed. However, the neglect of the possibility of a slight variation in the mirror reflectance coefficient with polarization may render this close agreement fortuitous. The second term in Eq. (38) will certainly increase with the power and at some point may cancel the nonlinearity responsible for the splitting in Eq. (45). It seems evident from the experimental results (Fig. 3) that this limit is not reached in the present case until more than three modes oscillate.

The evaluation of Eq. (45) for more than three holes is straightforward and not terribly interesting. As the nonlinearity contained in Eq. (45) implies, the splitting increases with the number of modes which go into oscillation. In general, the number of components at  $n(c/2L)$  is  $(N-n)$  where  $N$  is the number of holes ( $N \geq n$ ) and these components will not be spaced with perfect evenness. In each case, the absolute frequency of the component increases with the pumping rate if the hole repulsion effect predominates. For a symmetric distribution of holes about the Doppler line, the number of components at  $n(c/2L)$  is reduced.

#### 14. CONCLUSION

There exists one perplexing aspect of the hole burning interpretation which should be mentioned. At the highest power levels shown in Fig. 3, the odd-symmetric modes also go into oscillation, as evidenced by the appearance of the 1-Mc/sec satellites in Fig. 2. (These satellites are also split by amounts in the general order of 20 kc/sec.) A question naturally arises regarding the mechanism by which two modes separated by an amount substantially less than the natural linewidth can go into oscillation simultaneously. We note, however, that this question exists regardless of the inter-

pretation of the beat splitting. It seems probable that the answer to this question lies in the different spatial distributions of the two modes.

The main interest in the beat splitting phenomenon, of course, arises from the possibility of using this phenomenon to make an absolute frequency standard in the optical range. As mentioned in Sec. 3, this might be accomplished by the generation of an error frequency in the case of three oscillating modes and the use of this error frequency to adjust the plate separation. The central resonance may then be filtered out with a suitably designed (low quality) Fabry-Perot interferometer. It seems likely from the data in Sec. 3 that this error frequency would be in the general order of about 0.5 kc/sec per Mc/sec separation of the central cavity resonances from the center of the Doppler line and that the sharpness<sup>2,11</sup> of the maser oscillation would not be a prime limitation on the absolute stability obtainable in practice. Throughout the present analysis it has been assumed that the line shape for the transition is symmetric. This assumption will obviously break down at some point, and it is likely that the ultimate limit would be determined by pressure-dependent effects. The presence of other isotopes of neon can introduce such line asymmetries and it would obviously be desirable to isolate one of these isotopes for use in such a standard. From Thomas' numerical calculations and the natural abundance of Ne<sup>22</sup> in Ne<sup>20</sup>, the main effect of this line asymmetry would be to introduce a power-dependent frequency shift at the Doppler center in the order of 30 kc/sec. The presence of other isotopes of neon will also result in slight changes in the nonlinear part of the phase characteristic. In this connection it should be mentioned that no significant difference was found in either the mode pulling or beat splitting effects when the present maser was operated on a neon sample containing 99.9% Ne<sup>20</sup> as opposed to neon samples containing the normal isotopic abundance.

There are two more important sources of practical difficulty in utilizing the beat splitting effect to determine the absolute frequency of the central mode in respect to the Doppler center. The first consists of the possibility that the mirror reflectance coefficient may vary slightly with polarization.<sup>8</sup> If two modes were polarized in one direction and the third orthogonally, this effect could introduce an additional shift in the beat splitting. The effect enters by changing the hole depth and therefore the magnitude of the hole repulsion term. From Eq. (45) the shift in the splitting would amount to about  $\frac{3}{8}\Delta\nu_c(2LH/c)\Delta f/f$ , where  $\Delta f$  is the extreme variation of the fractional loss between the two orientations and  $H$  is the width of the hole for the orthogonally polarized mode. For example, for a hole width of 100 Mc/sec, a 1% variation in the mirror losses between the two extreme orientations would shift the beat splitting by about 2 kc/sec. Second, it has been found by others<sup>9,10</sup> using different observational techniques that the difference frequency between the two  $c/2L$  compo-

nents [Fig. 3(b)] jumps discontinuously to zero at some point below about 1 kc/sec. Under these conditions the  $2c/2L$  and  $c/2L$  beats are both harmonically related<sup>9</sup> and phase-locked<sup>10</sup> to a very high degree. Hence one completely loses track of the absolute frequencies at this point and it seems apparent that a minimum absolute frequency uncertainty in the order of 2 Mc/sec will exist. This effect is definitely not contained in Eq. (45). Although Eq. (45) does contain a slight nonlinear dependence on  $(\nu_m - \nu_1)$ , the nonlinear terms are much too small to give, for example, a cubic equation with real roots or a point of inflection near the origin. The effect probably has its origin in nonlinear time-dependent properties of the medium, which, as previously stated, have been neglected for reasons of simplicity.

Neither of these effects would prevent one from using the beat splitting phenomenon to obtain a high degree of relative frequency stabilization when the central mode is slightly detuned from the Doppler center.

#### ACKNOWLEDGMENTS

The author is particularly indebted to A. J. Rack for the use of his frequency measuring apparatus and help in obtaining the data in Table I. It is also a pleasure to acknowledge the help of D. E. Thomas for his numerical phase shift calculations and the technical assistance of P. Kindlmann. The author is also indebted to Professor W. W. Watson of Yale University for supplying the highly pure Ne<sup>20</sup> sample used. In addition, the author has benefitted from helpful discussions with Dr. W. L. Faust, Dr. C. G. B. Garrett, Dr. A. Javan, and Dr. J. A. White.

#### APPENDIX I

The phase shifts associated with a given line shape may be calculated most generally using methods equivalent to the Kramers-Kronig relations.<sup>15</sup> The assumptions on the following derivation are that the process obeys causality (i.e., the amplitude gain function is analytic in the lower half of the complex  $\omega$  plane), that the gain is small, and that the running wave is amplified linearly as it traverses the cavity. Although the gain saturates in the system during oscillation, we assume that amplification by this saturated gain characteristic is still linear.

We let  $K(\omega)$  be the complex, fractional amplitude gain in the medium defined by

$$1 + K(\omega) = [1 + K_0(\omega)] \exp[-i\phi(\omega)], \quad (\text{I.1})$$

where  $K_0(\omega)$  is the fractional amplitude gain per pass and  $\phi(\omega)$  is the additional single-pass phase shift resulting from the amplifying medium. Taking the logarithm of (I.1) and expanding in the limits  $K(\omega)$ ,  $K_0(\omega) \ll 1$ ,

$$K(\omega) \cong K_0(\omega) - i\phi(\omega). \quad (\text{I.2})$$

We note at this point that the fractional energy gain

per pass,  $g_0(\omega)$ , is

$$g_0(\omega) \cong 2K_0(\omega). \quad (\text{I.3})$$

We assume  $K(\omega)$  vanishes at  $\omega = \pm \infty$ ,  $\pm i \infty$ , and has no singularities in the lower half-plane. Then

$$\oint \frac{K(\omega)d\omega}{\omega - \omega_0} = 0, \quad (\text{I.4})$$

where the integral is taken along the real axis, skirts under the pole at  $\omega_0$  and is closed in the lower half of the complex  $\omega$  plane. Substituting (I.2) and equating real parts,

$$\phi(\omega_0) = - (1/\pi) \int_{-\infty}^{+\infty} \frac{K_0(\omega)d\omega}{\omega - \omega_0}, \quad (\text{I.5})$$

where (I.5) represents the principal part of the integral on the real axis. Equation (I.5) is more convenient for the Lorentzian than the usual form of the Kramers-Kronig relations deduced from it.

We take for the Lorentzian,

$$K_0(\omega) \cong K_m(\Delta\omega)^2 [(\Delta\omega)^2 + 4(\omega_m - \omega)^2]^{-1} \quad (\text{I.6})$$

where the approximation  $\omega + \omega_m \cong 2\omega$  has been made. Although  $K_0(\omega)$  has a pole in the lower half-plane,  $K(\omega)$  does not. We next take,

$$I = \oint \frac{K_0(\omega)d\omega}{\omega - \omega_0}, \quad (\text{I.7})$$

where the path of integration runs along the real axis, skirts under the pole at  $\omega_0$  and is closed in the upper half-plane. From (I.5), (I.6), and (I.7),

$$-\pi\phi(\omega_0) + \pi i K_0(\omega_0) = 2\pi i \sum (\text{Residues}). \quad (\text{I.8})$$

Hence,

$$\begin{aligned} \phi(\omega_0) &= -2K_0(\omega_0)(\omega_m - \omega_0)/\Delta\omega \\ &= -g_0(\omega_0)(\omega_m - \omega_0)/\Delta\omega \end{aligned} \quad (\text{I.9})$$

yielding Eq. (11) of the text.

#### APPENDIX II

The hole widths may be evaluated through a standard application of time-dependent perturbation theory.<sup>20</sup> We assume that the two maser levels are described by the wave function

$$\Psi(r, t) = A\psi_a + B\psi_b. \quad (\text{II.1})$$

Satisfying

$$(H_0 + H')\Psi = i\hbar\partial\Psi/\partial t \quad (\text{II.2})$$

in the presence of the electromagnetic field.  $H_0$  is the original Hamiltonian and  $H'$  the time-dependent per-

<sup>20</sup> A similar analysis for levels having different decay rates has been given for the ground state of positronium by V. W. Hughes, S. Marder, and C. S. Wu [Phys. Rev. **106**, 934 (1957), Appendix I]. The approximation,  $\gamma_b \gg \gamma_a$ , appropriate to the latter reference has, however, not been made here.

turbation. The subscript "a" denotes the upper maser level and "b" the lower. The probability amplitudes  $A$  and  $B$  are functions of the time. We take the electric field to be linearly polarized in the  $z$  direction. Hence,

$$H' = -ezE_0 \cos \omega t = -(ezE_0/2)(e^{i\omega t} + e^{-i\omega t}). \quad (\text{II.3})$$

Since the perturbation is electric dipole in nature, only off-diagonal matrix elements arise. Neglecting the anti-resonant term and the interaction with all neighboring levels,

$$\begin{aligned} \dot{A} &= (V/i\hbar)e^{-i(\omega-\omega_0)t} - (\gamma_a/2)A, \\ \dot{B} &= (V/i\hbar)e^{i(\omega-\omega_0)t} - (\gamma_b/2)B, \end{aligned} \quad (\text{II.4})$$

where the spontaneous decay rates  $\gamma_a$  and  $\gamma_b$  of the upper and lower maser levels have been introduced phenomenologically. From (II.3)

$$V = -\frac{1}{2}eE_0(z)_{a,b}. \quad (\text{II.5})$$

$\omega_0$  represents the resonant frequency of the atomic transition and  $\omega$  the frequency of the oscillating field.

We seek those solutions to the coupled Eqs. (II.4) satisfying the initial conditions

$$A=1 \quad \text{and} \quad B=0 \quad \text{at} \quad t=0. \quad (\text{II.6})$$

Condition (II.6) corresponds to putting the atom in the upper state at  $t=0$ . The total probability that the atom decays by stimulated emission is then given by

$$P_s = \gamma_b \int_0^\infty |B(t)|^2 dt. \quad (\text{II.7})$$

Through standard methods, the solution of Eqs. (II.4) for  $B(t)$  subject to initial conditions (II.6) is

$$B(t) = \frac{i\hbar}{V} \frac{(\mu_- + \frac{1}{2}\gamma_a)(\mu_+ + \frac{1}{2}\gamma_a)}{(\mu_+ - \mu_-)} [e^{\mu_- t} - e^{\mu_+ t}] e^{i(\omega-\omega_0)t}, \quad (\text{II.8})$$

where

$$\begin{aligned} \mu_\pm &= -\frac{1}{2} \left[ \frac{1}{2}(\gamma_a + \gamma_b) + i(\omega - \omega_0) \right] \\ &\quad \pm \frac{1}{2} \left\{ \left[ \frac{1}{2}(\gamma_b - \gamma_a) + i(\omega - \omega_0) \right]^2 - |2V/\hbar|^2 \right\}^{1/2}. \end{aligned} \quad (\text{II.9})$$

Hence

$$\begin{aligned} P_s &= \gamma_b \left| \frac{\hbar}{V} \right|^2 \left| \frac{(\mu_- + \frac{1}{2}\gamma_a)(\mu_+ + \frac{1}{2}\gamma_a)}{(\mu_+ - \mu_-)} \right|^2 \\ &\quad \times \int_0^\infty |e^{\mu_- t} - e^{\mu_+ t}|^2 dt. \end{aligned} \quad (\text{II.10})$$

After some algebraic manipulation, Eq. (II.10) reduces to

$$P_s = \frac{\gamma_b(\gamma_a + \gamma_b) |2V/\hbar|^2}{4(\omega - \omega_0)^2 \gamma_a \gamma_b + (\gamma_a \gamma_b + |2V/\hbar|^2)(\gamma_a + \gamma_b)^2}, \quad (\text{II.11})$$

yielding Eq. (27) of the text.<sup>21</sup> Aside from the minor approximations made in formulating Eqs. (II.4), this expression for the probability function is exact.

<sup>21</sup> Note added in proof. A result equivalent to Eq. (II.11) has been obtained from the density matrix method by W. E. Lamb, Jr., and T. M. Sanders, Jr., Phys. Rev. **119**, 1901 (1960).

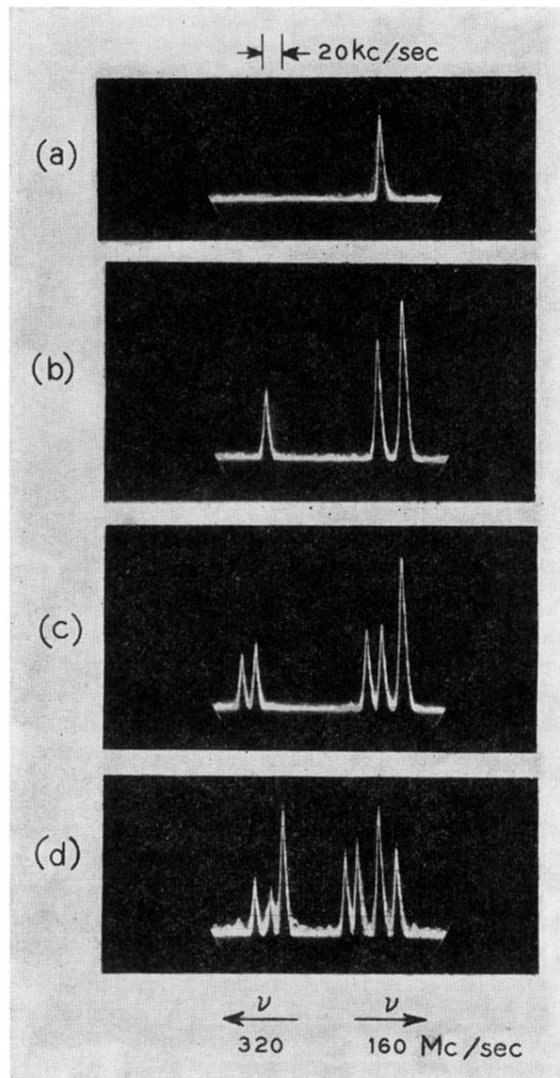


FIG. 3. Splitting of  $c/2L$  and  $2(c/2L)$  beats with power. Power increases from (a) to (d).